Water-wave gap solitons: An approximate theory and numerical solutions of the exact equations of motion

V. P. Ruban*

Landau Institute for Theoretical Physics, 2 Kosygin Street, 119334 Moscow, Russia

(Received 15 July 2008; revised manuscript received 30 October 2008; published 17 December 2008)

It is demonstrated that a standard coupled-mode theory can successfully describe weakly nonlinear gravity water waves in Bragg resonance with a periodic one-dimensional topography. Analytical solutions for gap solitons provided by this theory are in reasonable agreement with numerical simulations of the exact equations of motion for ideal planar potential free-surface flows, even for strongly nonlinear waves. In numerical experiments, self-localized groups of nearly standing water waves can exist up to hundreds of wave periods. Generalizations of the model to the three-dimensional case are also derived.

DOI: 10.1103/PhysRevE.78.066308 PACS number(s): 47.15.K−, 47.35.Bb, 47.35.Lf

I. INTRODUCTION

As we know from nonlinear optics, specific self-localized waves can propagate in periodic nonlinear media, with a frequency inside the spectrum gap. These waves are referred to as gap solitons (alternatively called Bragg solitons; see, e.g., Refs. [1–11]). In the field of Bose-Einstein condensation also, gap solitons (GSs) are known [12–14]. Recently, it has been realized that GSs are also possible in water-wave systems [15]. In particular, very accurate numerical experiments have shown that finite-amplitude standing waves over a periodic one-dimensional topography are subjected to a modulational instability which spontaneously produces Bragg quasisolitons—localized coherent structures existing for dozens of wave periods. However, in the cited work [15], no analytical approach was presented. As a result, many important questions about the shape and stability of water-wave GSs were not answered. The present work is intended to clarify this issue, at least partly. More specifically, for a given periodic bottom profile with a spatial period Λ, we shall derive, in some approximation, coefficients for a standard model system of two coupled equations, describing evolution of the forward- and backward-propagating wave envelopes $A_{\pm}(x,t)$ (see, e.g., Refs. [2,4,7,10]),

$$i(\partial_t \pm V_g \partial_x)A_{\pm} = \Delta A_{\mp} + (\Gamma_S|A_{\pm}|^2 + \Gamma_X|A_{\mp}|^2)A_{\pm}, \qquad (1)$$

where t is the time, x is the horizontal coordinate in the flow plane, and $A_{\pm}(x,t)$ are slow functions. Let the free surface be at $y=0$ at equilibrium. Then elevation of the surface $y=\eta(x,t)$ is given by the following formula:

$$\eta(x,t) = \mathrm{Re}(A_+ e^{i\kappa x - i\omega_0(\kappa)t} + A_- e^{-i\kappa x - i\omega_0(\kappa)t}) + (\text{higher-order terms in } \kappa A_{\pm}), \qquad (2)$$

where $\kappa = 2\pi/(2\Lambda)$ is the wave number corresponding to the main Bragg resonance, $\omega_0(\kappa) = [g\kappa \tanh(h_0\kappa)]^{1/2}$ is the frequency at the gap center, g is the gravity acceleration, and h_0 is the effective depth of the water canal [definitely, h_0 is not a mean depth; more precisely it will be specified later by Eqs. (6) and (7)]. The coefficients in Eqs. (1) are the effective group velocity $V_g = d\omega_0(\kappa)/d\kappa$, the half-width Δ of the frequency gap, the nonlinear self-interaction Γ_S, and the nonlinear cross interaction Γ_X.

Generally, the following assumptions are made in derivation of the above simplified standard model. (a) Dissipative processes are negligible. (b) The periodic inhomogeneity is relatively weak (that is, $\Delta \ll \omega_0$). (c) The waves are weakly nonlinear. (d) The original (without inhomogeneity) equations of motion, when written in terms of normal complex variables $A_{\mathbf{k}}$, contain nonlinearities starting from the order 3:

$$i\dot{A}_{\mathbf{k}} \approx \omega_*(\mathbf{k})A_{\mathbf{k}} + \frac{1}{2}\int T(\mathbf{k},\mathbf{k}_2;\mathbf{k}_3,\mathbf{k}_4)A^*_{\mathbf{k}_2}A_{\mathbf{k}_3}A_{\mathbf{k}_4} \times \delta(\mathbf{k}+\mathbf{k}_2-\mathbf{k}_3-\mathbf{k}_4)d\mathbf{k}_2 d\mathbf{k}_3 d\mathbf{k}_4, \qquad (3)$$

where $\omega_*(\mathbf{k})$ is a linear dispersion relation in the absence of periodic inhomogeneity [a weak inhomogeneity adds some small terms to the right-hand side of Eq. (3); the most important effect arises from a term $\hat{L}A_{\mathbf{k}}$, where $\hat{L}$ is a "small" linear nondiagonal operator]. It is also required that (e) the coefficient $T(\mathbf{k}_1,\mathbf{k}_2;\mathbf{k}_3,\mathbf{k}_4)$ of the four-wave nonlinear interaction should be a continuous function. In application to water waves the requirements (d) and (e) mean that (i) all the second-order nonlinearities are assumed to be excluded by a suitable canonical transformation (the corresponding procedure is described, e.g., in Refs. [16,17]); (ii) the model system (1) can be good only in the limit of relatively deep water, since at a finite depth the function $T(\mathbf{k}_1,\mathbf{k}_2;\mathbf{k}_3,\mathbf{k}_4)$ is known to contain discontinuities which disappear at infinite depth (see, e.g., Ref. [17]). Therefore we introduce a small parameter

$$\varepsilon \equiv \exp(-2\kappa h_0) \ll 1, \qquad (4)$$

and we consider in the main approximation only the principal effect of weak spatial periodicity, namely, creation of a narrow frequency gap with $\Delta \sim \varepsilon\omega_0$ under the main Bragg resonance conditions. Then we imply a standard procedure for obtaining approximate equations for slow wave envelopes, where the deep-water limit of $T(\mathbf{k}_1,\mathbf{k}_2;\mathbf{k}_3,\mathbf{k}_4)$ is used for the coefficients $\Gamma_S \propto T(\kappa,\kappa;\kappa,\kappa)$ and $\Gamma_X \propto 2T(\kappa,-\kappa;\kappa,-\kappa)$. Thus we neglect in the actual nonlinear

*ruban@itp.ac.ru

wave interaction some relatively small terms with coefficients of order ε.

Of course, the functions $A_{\pm}$ should be sufficiently "narrow" in the Fourier space, since dispersive terms proportional to second-order derivatives $\partial_x^2 A_{\pm}$ are not included in the model.

After derivation of all the coefficients in Sec. II, some known "solitonic" solutions of Eqs. (1) will be compared to numerical results for exact hydrodynamic equations, with nearly the same initial conditions as for the solitons (in Sec. III). We shall see that very long-lived self-localized groups of standing water waves are possible. In some region of soliton parameters, water-wave GSs exist up to hundreds of wave periods, until processes not included in Eq. (1) change them significantly. In Sec. IV we discuss some promising directions of further research, concerning three-dimensional generalizations of the coupled mode equations. Some auxiliary calculations are placed in two Appendixes.

II. COEFFICIENTS OF THE MODEL

We start our consideration with a short discussion of the conditions when dissipation due to bottom friction, caused by water's (kinematic) viscosity ν, is not important in the wave dynamics. Obviously, the viscous sublayer should be relatively thin in this case: $d_b \ll \Lambda$. In the nearly linear regime, the width of the sublayer can be estimated as $d_b \sim (\nu/\omega)^{1/2}$, where $\omega \sim (g/\Lambda)^{1/2}$. This gives us the following necessary condition for applicability of the conservative theory:

$$\Lambda^{3/4} g^{1/4} \nu^{-1/2} \gg 1. \tag{5}$$

Generally speaking, one cannot exclude the possibility that in a strongly nonlinear regime the vorticity can sometimes be advected by a wave-produced alternating velocity field far away from the rigid bottom boundary. Such vortex structures are typically generated near curved parts of the bed, and they can significantly interact with surface waves. However, we assume this is not the case; otherwise, the problem becomes too complicated. Although we do not have a simple criterion to evaluate the influence of the bottom-produced vorticity, with $\Lambda \gtrsim 1$ m we still hope to be correct when neglecting water viscosity, as well as compressibility and surface tension. This allows us to exploit the model of purely potential free-surface ideal fluid flows, commonly used in the water-wave theory.

Since in this work we consider the case of relatively deep water, we can write $\omega_0(\kappa) \approx \omega_*(\kappa)(1-\varepsilon)$, where $\omega_*(\kappa) = (g\kappa)^{1/2}$ is the frequency corresponding to infinite depth. Later we will see that the values $\varepsilon = 0.01-0.02$ are of the most interest.

Let us introduce conformal curvilinear coordinates (ζ_1, ζ_2) determined by an analytic function $\mathcal{B}(\tilde{\zeta})$, with $\tilde{\zeta} = \zeta_1 + i(\zeta_2 - h_0)$, so that

$$x + iy = \mathcal{B}(\tilde{\zeta}) = \tilde{\zeta} - 2\kappa^{-1} \sum_{n=1}^{\infty} \beta_n \varepsilon^n \sin(2n\kappa\tilde{\zeta}), \tag{6}$$

with real coefficients β_n. Without loss of generality, we assume $\beta_1 > 0$. The unperturbed water surface $y=0$ corresponds to real values of $\tilde{\zeta} = \zeta_1 - i0$, while at the bottom we have $\zeta_2 = 0$, and

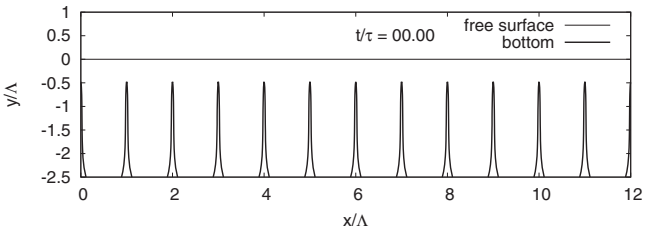

FIG. 1. Example I: unperturbed free surface and the bottom profile for $2h_0\kappa = 1.4\pi$, $D_0 = 0.95$, and $\varepsilon C = 0.012\,29$ [see Eq. (21)].

$$X^{(b)}(\zeta_1) + iY^{(b)}(\zeta_1) = \mathcal{B}(\zeta_1 - ih_0) \tag{7}$$

is a parametric representation of the bed profile, which can be highly undulating (see, for example, Fig. 1).

In these conformal coordinates, a spectrum $\omega(\mu)$ of linear potential waves is determined through the following equation (compare to Ref. [18], where an analogous approach but slightly different notations were used):

$$[\omega^2 \mathcal{B}'(\zeta_1) - g\hat{k}\tanh(h_0\hat{k})]\Psi_\mu(\zeta_1) = 0, \tag{8}$$

with

$$\mathcal{B}'(\zeta_1) = 1 - 4\sum_{n=1}^{\infty} n\beta_n \varepsilon^n \cos(2n\kappa\zeta_1). \tag{9}$$

Here $[\hat{k}\tanh(h_0\hat{k})]$ is a linear operator which is diagonal in Fourier representation: for any function $f(\zeta_1) = \int f_k \exp(ik\zeta_1)dk/2\pi$ we have

$$[\hat{k}\tanh(h_0\hat{k})]f(\zeta_1) = \int k\tanh(h_0k) f_k e^{ik\zeta_1} dk/2\pi. \tag{10}$$

The eigenfunction $\Psi_\mu(\zeta_1)$ takes the form

$$\Psi_\mu(\zeta_1) = e^{i\mu\zeta_1} \sum_{n=-\infty}^{+\infty} c_n e^{2in\kappa\zeta_1}, \tag{11}$$

with some coefficients c_n. With a given μ, we have an infinite homogeneous linear system of equations for c_n. Nontrivial solutions exist for some discrete values $\omega_{(m)}(\mu)$. The first gap in the spectrum is the difference between the two first eigenvalues at $\mu = \kappa$, that is, $2\Delta = \omega_{(2)}(\kappa) - \omega_{(1)}(\kappa)$. Approximately, for small ε these eigenvalues are determined by the coefficient β_1 (compare to Ref. [18]),

$$\omega_{(1,2)}^2(\kappa) \approx g\kappa\tanh(h_0\kappa)(1 \mp 2\varepsilon\beta_1). \tag{12}$$

It should be noted that $\omega_{(1)}(\kappa)$ corresponds to $\Psi_\kappa^{(1)} \approx \sin(\kappa\zeta_1)$, while $\omega_{(2)}(\kappa)$ corresponds to $\Psi_\kappa^{(2)} \approx \cos(\kappa\zeta_1)$. Thus, in the first order in ε, the half-width Δ of the gap in the spectrum of linear waves is

$$\Delta \approx \omega_*(\kappa)\varepsilon\beta_1 \equiv \omega_*(\kappa)\tilde{\Delta}, \tag{13}$$

where $\tilde{\Delta} = \varepsilon\beta_1 \ll 1$ is a small dimensionless quantity.

As to the nonlinearity coefficients Γ_S and Γ_X, their values for the case of infinite depth (in other words, their zeroth-

order approximations in ε) can be easily extracted from Ref. [19]:

$$\Gamma_S \approx \frac{1}{2}\omega_*(\kappa)\kappa^2, \quad \Gamma_X \approx -\omega_*(\kappa)\kappa^2. \tag{14}$$

It should be noted that the cited work [19] relies on results obtained earlier by Krasitskii [16], who calculated the kernels of the so-called reduced integro-differential equation for weakly nonlinear surface water waves (see also the paper by Zakharov [17], and references therein). It is important in many aspects that for deep-water waves the coefficients Γ_S and Γ_X have the opposite signs, and their ratio is $\Gamma_S/\Gamma_X \approx -1/2$.

With the same zeroth-order accuracy, the group velocity is

$$V_g \approx \frac{1}{2}\frac{\omega_*(\kappa)}{\kappa}. \tag{15}$$

Now all the coefficients have been derived, and the simplified coupled-mode equations for relatively deep-water waves in Bragg resonance with a periodic bottom take the following explicit form:

$$i\left(\frac{\partial_t}{\omega_*} + \frac{\partial_x}{2\kappa}\right)a_+ = \tilde{\Delta}a_- + \frac{1}{2}(|a_+|^2 - 2|a_-|^2)a_+, \tag{16}$$

$$i\left(\frac{\partial_t}{\omega_*} - \frac{\partial_x}{2\kappa}\right)a_- = \tilde{\Delta}a_+ + \frac{1}{2}(|a_-|^2 - 2|a_+|^2)a_-, \tag{17}$$

where $a_\pm(x,t) = \kappa A_\pm(x,t)$ are dimensionless wave amplitudes. Analytical solutions are known for the above system (see [2,4,7,10]), describing moving localized structures, the gap solitons. In the simplest case the velocity of GSs is zero, and the solutions essentially depend on a parameter δ, the relative frequency inside the gap $(-1 < \delta < 1)$:

$$a_\pm = \sqrt{I(x)}\exp[-i\delta\tilde{\Delta}\omega_* t + i\gamma_0 \pm i\varphi(x)], \tag{18}$$

$$I(x) = \frac{4\tilde{\Delta}(1-\delta^2)}{\cosh(4\tilde{\Delta}\sqrt{1-\delta^2}\kappa x) + \delta}, \tag{19}$$

$$\varphi(x) = \arctan\left(\sqrt{\frac{1-\delta}{1+\delta}}\tanh(2\tilde{\Delta}\sqrt{1-\delta^2}\kappa x)\right). \tag{20}$$

These expressions correspond to purely standing, spatially localized waves with frequency $\omega = (1 - \varepsilon + \delta\tilde{\Delta})\omega_*$ (concerning their stability, see Ref. [7], where, however, stability domains were presented for a different ratio Γ_S/Γ_X; there are some numerical indications that the above GSs are stable in the parametric interval $\delta_* < \delta < 1$, where the critical value $\delta_* \approx -0.4$).

It should be noted that one can hardly expect a detailed correspondence between the very simple model (16) and (17) and the fully nonlinear dynamics, but just a general accordance sometimes is possible. In particular, the model does not describe nonlinear processes resulting in generation of short waves which take the wave energy away from a soliton, thus influencing its dynamics. The model is also not generally good for studying collisions between solitons, since the wave amplitude can significantly increase in intermediate states.

III. NUMERICAL EXPERIMENTS

In order to compare the above approximate analytical solutions to nearly exact numerical solutions, we chose the following function $\mathcal{B}(\tilde{\zeta})$:

$$\mathcal{B}(\tilde{\zeta}) = \tilde{\zeta} + \frac{iD_0}{\kappa}\ln\left(\frac{1 + \varepsilon C e^{2i\kappa\tilde{\zeta}}}{1 + \varepsilon C e^{-2i\kappa\tilde{\zeta}}}\right), \tag{21}$$

with real parameters $0 < D_0 < 1$, and $0 < C < 1$. Hence, $\tilde{\Delta} = \varepsilon D_0 C < \varepsilon$. For D_0 and C both close to 1, Eq. (21) gives periodically arranged barriers (see, for example, Fig. 1). The barriers are relatively thin when $(1 - D_0) \ll 1$, and relatively high as $C \to 1$. However, in numerical experiments with high-amplitude waves, a strong tendency was noticed toward formation of sharp wave crests over very thin barriers (say, when $D_0 = 0.99$), already after a few wave periods. With sharp crests, the conservative potential-flow-based model fails (it is also clear that the tops of narrow barriers must generate strong vortex structures). Therefore we took $D_0 = (0.7-0.9)$ in most of our computations in order to have a smooth surface for a longer time. Exact equations for ideal potential free-surface planar flows were simulated (their derivation can be found in Ref. [18]; some generalizations are made in Refs. [20,21]). As in Ref. [15], we dealt with dimensionless variables corresponding to $\tilde{g} = 1$, $\tilde{\kappa} = 100$. The dimensionless time $\tilde{t}$ is then related to the physical time $t = \tau\tilde{t}$ by a factor $\tau = (100\Lambda/\pi g)^{1/2}$. For instance, the period of linear deep-water waves with the length $\lambda = 2\Lambda$ is $T_* = (2\pi/\sqrt{100})\tau \approx 0.628\tau$. At $t = 0$, we set the horizontal free surface, while the initial distribution of the surface-value velocity potential was

$$\psi_0(\zeta_1) = 2\kappa^{-3/2}\sqrt{I(\zeta_1)}\cos[\kappa\zeta_1 + \varphi(\zeta_1)] \approx \Psi_{\mathrm{GS}}(\zeta_1), \tag{22}$$

in accordance with the approximate relation $\eta_t \approx \kappa\psi$.

Many simulations with different parameters were performed, and a very good general agreement was found between numerical and analytical results in the weakly nonlinear case, that is, for small steepness $s \equiv 2[I(0)]^{1/2} = 4[\tilde{\Delta}(1-\delta)]^{1/2} \lessapprox 0.35$. So, with $2h_0\kappa = 1.4\pi$, $D_0 = 0.95$, $\varepsilon C = 0.012\,29$, and $\delta = 0.4$ (example I), some noticeable deviations from the purely-standing-wave regime were observed only after $t/\tau \gtrsim 120$ (see Figs. 2 and 3). In a real-world experiment it could be several minutes with $\Lambda \sim 1$ m.

It is interesting that, even for larger s, up to $s \approx 0.48$, GSs can exist for dozens of wave periods. A numerical example for such a relatively high-amplitude water-wave GS is presented in Figs. 4 and 5, where $2h_0\kappa = 1.2\pi$, $D_0 = 0.7$, $\varepsilon C = 0.022$, and $\delta = 0.0$ (example II). In this simulation, there were 45 oscillations before sharp crest formation (see Figs. 4 and 6). As to a further evolution of such GSs, only in a

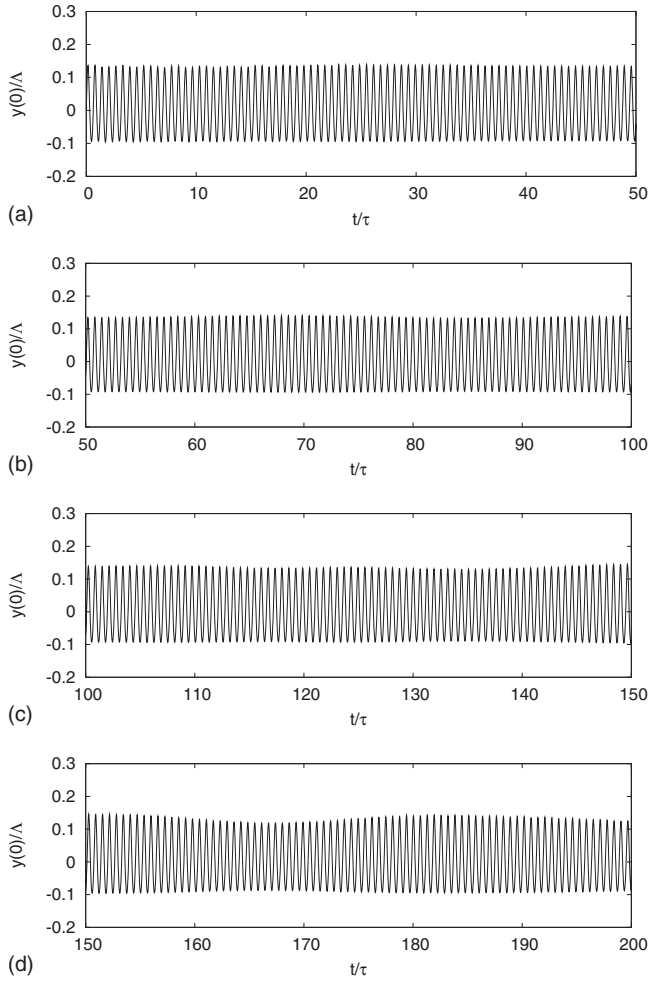

FIG. 2. Example I: free-surface elevation at $x=0$ (at the center of a GS) for $\delta=0.4$.

real-world experiment will it be possible to get reliable knowledge about it, since various dissipative processes come into play.

Concerning water-wave GSs with negative δ, their behavior for $\delta>-0.4$ was found stable, while for $\delta\leqslant-0.5$ the dynamics was unstable, and partial disintegration of GSs was observed after a few tens of wave periods (not shown). However, in some numerical experiments, the lifetime of GSs was limited by the above-mentioned process of sharp crest formation rather than by their own instability in the frame of the model (16) and (17), at least with $s\gtrapprox0.4$ (not shown).

Finally, we would like to present an example of interaction of two GSs (example III). The bed parameters are $2h_0\kappa=1.2\pi$, $D_0=0.7$, and $\varepsilon C=0.023$. Both solitons initially had $\delta=0.4$ and they were separated by a distance 66Λ. At $t=0$ we set the horizontal free surface and

$$\psi_0(\zeta_1)\approx\Psi_{\mathrm{GS}}(\zeta_1-33\Lambda)+\Psi_{\mathrm{GS}}(\zeta_1+33\Lambda). \qquad (23)$$

This numerical experiment also describes interaction of a single GS with a vertical wall at $x=0$. Surface profiles for several time moments are shown in Figs. 7 and 8. We see that in this example the interaction between GSs is attractive.

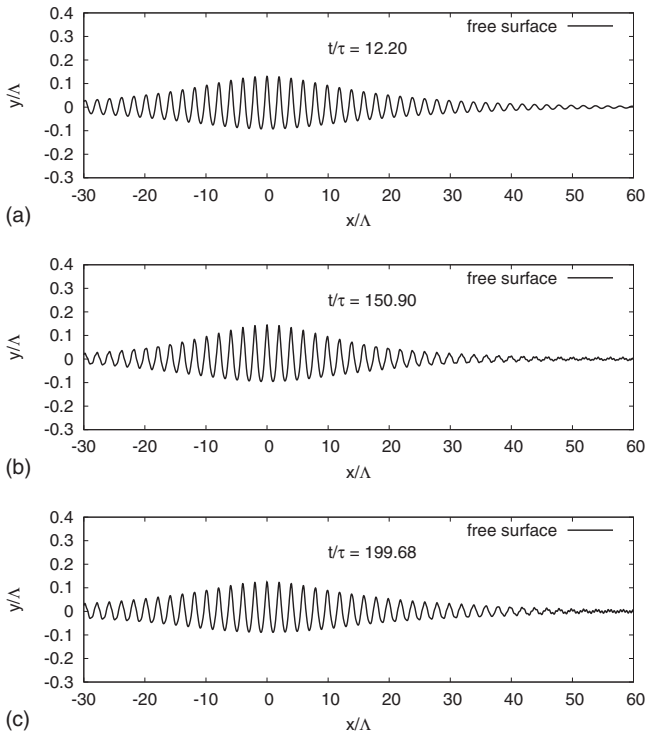

FIG. 3. Example I: free-surface profiles for different time moments when elevation at $x=0$ is at a maximum.

They collide and produce a highly nonlinear and short wave group near $x=0$.

IV. THREE-DIMENSIONAL GENERALIZATIONS AND DISCUSSION

In this work, coefficients of the standard model (1) were derived for water-wave GSs in the approximation of relatively deep water. The frequency gap in this case is small (of order ε) despite strong bed undulations. It seems that a more general situation of intermediate depth cannot be described by this basic model, since an interaction of the main wave with a long-scale flow ("zeroth harmonics") is then essential and should be included in the equations. At the formal level, this corresponds to the mentioned discontinuities of the four-wave matrix element $T(\mathbf{k}_1,\mathbf{k}_2;\mathbf{k}_3,\mathbf{k}_4)$ at a finite depth. Actually, in finite-depth dynamics, three-wave interactions are more essential, and therefore they cannot be removed efficiently by a weakly nonlinear transformation. This is the main difference between the present third-order theory and

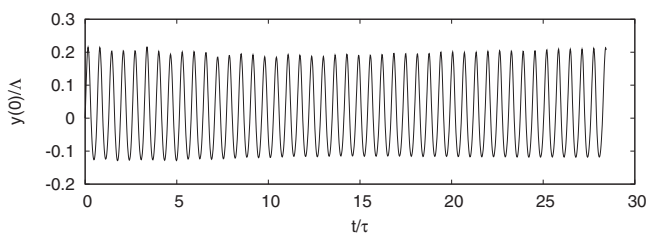

FIG. 4. Example II: free-surface elevation at $x=0$ for $2h_0\kappa=1.2\pi$, $D_0=0.7$, $\varepsilon C=0.022$, and $\delta=0.0$.

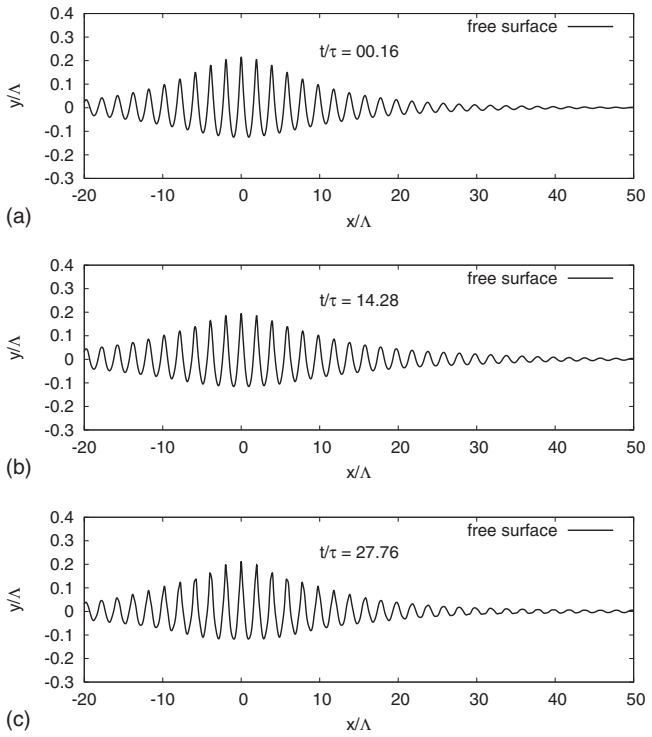

FIG. 5. Example II: free-surface profiles for different time moments corresponding to maximum elevation at $x=0$.

previously developed second-order theories (see, for example, Ref. [22]).

So far we have considered purely two-dimensional flows, with the single horizontal coordinate x. Let us now introduce two important generalizations for three-dimensional flows. Below we only derive the equations, but their detailed analysis will be a subject of future work.

In the first case, the bottom topography is still one dimensional, but we take into account weak variations of the wave field along the second horizontal coordinate q, simply by adding dispersive terms, proportional to $\partial_q^2 a_\pm$, to the coupled-mode system, as written below:

$$\left(\frac{i\partial_t}{\omega_*} \pm \frac{i\partial_x}{2\kappa} + \frac{\partial_q^2}{4\kappa^2}\right) a_\pm = \tilde{\Delta} a_\mp + \frac{1}{2}(|a_\pm|^2 - 2|a_\mp|^2) a_\pm . \tag{24}$$

In this system, a near-band-edge approximation for the upper branch of the linear spectrum gives a two-dimensional (2D) focusing nonlinear Schrödinger equation (NLSE). Thus, in the long-scale limit, the system (24) exhibits a tendency toward wave collapse which is known as a typical feature of 2D NLSE dynamics.

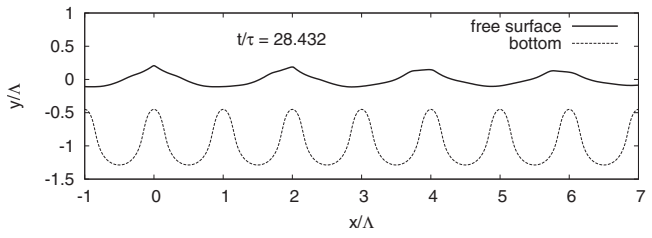

FIG. 6. Example II: formation of sharp wave crests over barriers.

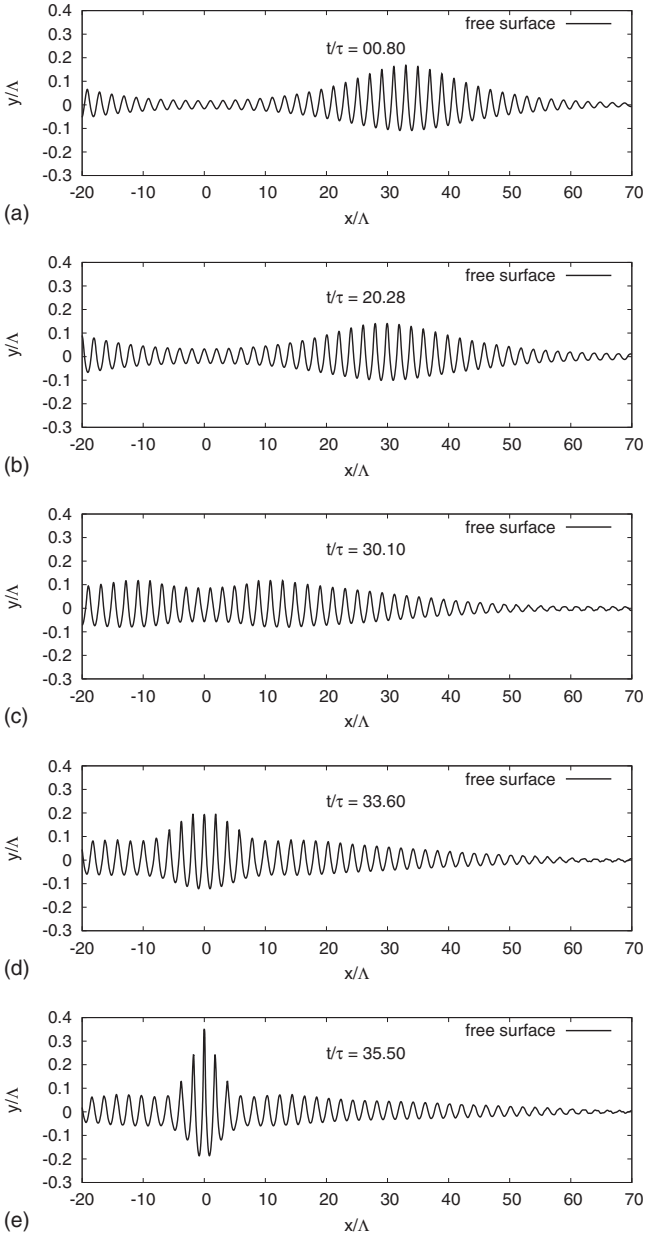

FIG. 7. Example III: interaction of two water-wave GSs.

In the second case, the periodic bottom profile $Y^{(b)}(x,q) = -h + \chi(x,q)$ is essentially two dimensional, and in the horizontal Fourier plane there are several pairs of Bragg-resonant wave vectors. For simplicity, we present below equations for the case when $\chi(x,q)$ has the symmetry of a square lattice, with equal periods Λ in both horizontal directions x and q:

$$\chi = \sum_{n_1 n_2} \alpha_{n_1 n_2} [\cos(2n_1 \kappa x + 2n_2 \kappa q) + \cos(2n_1 \kappa x - 2n_2 \kappa q)], \tag{25}$$

where the coefficients possess the symmetry $\alpha_{n_1 n_2} = \alpha_{n_2 n_1}$. Let us consider the interaction of two wave pairs having slow

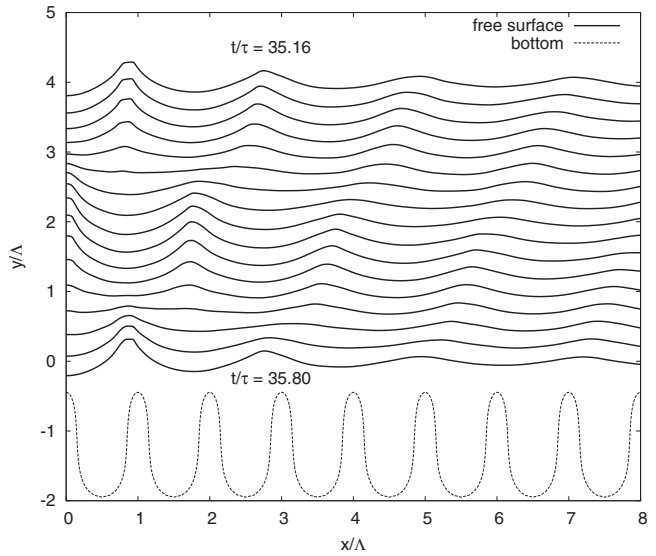

FIG. 8. Example III: highly nonlinear wave near $x=0$. Here the free-surface profiles are presented from $t/\tau=35.16$ to 35.80 with the time interval $\Delta t/\tau=0.04$. The wave profiles, except the last one, are given vertically shifted for convenience. The bed shape is also shown.

complex amplitudes $a_{\pm}(x,q,t)$ and $b_{\pm}(x,q,t)$, with the first pair corresponding to wave vectors $\pm\mathbf{p}_1=\pm(\pi/\Lambda)(1,1)$ and the second pair corresponding to $\pm\mathbf{p}_2=\pm(\pi/\Lambda)(-1,1)$. It is important that the absolute values are equal to each other: $|\mathbf{p}_1|=|\mathbf{p}_2|=\sqrt{2}\kappa\equiv\varkappa$. Again we will assume $\epsilon\equiv\exp(-2\varkappa h)\ll 1$. It is convenient to use new horizontal coordinates

$$x_1=\frac{q+x}{\sqrt{2}},\quad x_2=\frac{q-x}{\sqrt{2}}. \tag{26}$$

The elevation $y=\eta(x_1,x_2,t)$ of the free surface is then given by the formula

$$\varkappa\eta=\mathrm{Re}[e^{-i\Omega_0 t}(a_+e^{i\varkappa x_1}+a_-e^{-i\varkappa x_1}+b_+e^{i\varkappa x_2}+b_-e^{-i\varkappa x_2})]+\cdots, \tag{27}$$

where $\Omega_0=[g\varkappa\tanh(h_0\varkappa)]^{1/2}\approx\Omega_*(1-\epsilon_0)$, with $\Omega_*=(g\varkappa)^{1/2}$ and $\epsilon_0=\exp(-2\varkappa h_0)$, and the ellipsis corresponds to higher-order terms (again, we should note that generally $h_0\neq h$). The approximate equations of motion for the amplitudes have the form

$$i\left(\frac{\partial_t}{\Omega_*}\pm\frac{\partial_{x_1}}{2\varkappa}\right)a_{\pm}=\epsilon_1 a_{\mp}+\epsilon_2(b_++b_-)+\frac{\partial\mathcal{H}_{\mathrm{nl}}}{\partial a_{\pm}^*}, \tag{28}$$

$$i\left(\frac{\partial_t}{\Omega_*}\pm\frac{\partial_{x_2}}{2\varkappa}\right)b_{\pm}=\epsilon_1 b_{\mp}+\epsilon_2(a_++a_-)+\frac{\partial\mathcal{H}_{\mathrm{nl}}}{\partial b_{\pm}^*}, \tag{29}$$

where the small constants ϵ_1 and ϵ_2 depend on the given bed profile, $a_{\pm}^*$ and $b_{\pm}^*$ mean the complex conjugate quantities, and the function $\mathcal{H}_{\mathrm{nl}}$ corresponds to nonlinear interactions. Using an explicit expression from Ref. [17] for the deep-water four-wave resonant interaction $T(\mathbf{k}_1,\mathbf{k}_2;\mathbf{k}_3,\mathbf{k}_4)$, we have

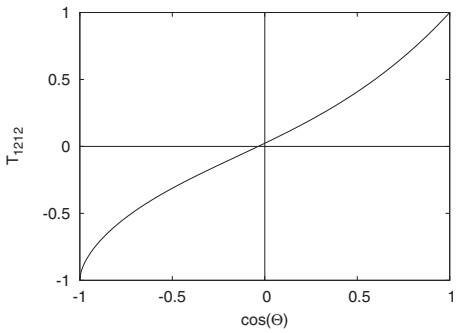

FIG. 9. Normalized matrix element $T(\mathbf{k}_1,\mathbf{k}_2;\mathbf{k}_1,\mathbf{k}_2)$ for two wave vectors of equal length, with an angle Θ between them.

$$\mathcal{H}_{\mathrm{nl}}=\frac{1}{4}\{|a_+|^4+|a_-|^4+|b_+|^4+|b_-|^4\}-|a_+|^2|a_-|^2-|b_+|^2|b_-|^2$$
$$+\tau_\perp\{|a_+|^2|b_+|^2+|a_+|^2|b_-|^2+|a_-|^2|b_+|^2+|a_-|^2|b_-|^2\}$$
$$-\frac{3}{4}(a_+a_-b_+^*b_-^*+a_+^*a_-^*b_+b_-), \tag{30}$$

where $\tau_\perp=T_{1212}(0)\approx 0.023\,46$ is the normalized value of the matrix element $T(\mathbf{k}_1,\mathbf{k}_2;\mathbf{k}_1,\mathbf{k}_2)$ for two perpendicular wave vectors of equal length (see Fig. 9). Since $\tau_\perp\ll 1$, we actually may neglect in $\mathcal{H}_{\mathrm{nl}}$ the terms proportional to $\tau_\perp$.

Unfortunately, it is hardly possible to find some analytical space-dependent solution for the nonlinear system (28) and (29), but it can be investigated by approximate methods. The parameters ϵ_0, ϵ_1, and ϵ_2 can in principle be calculated from solution of a linearized problem for water waves over a periodic 2D bed. An exact linearized equation for the surface value of the velocity potential can be written in the form

$$\{\omega^2/g-[\hat{k}\tanh(h\hat{k})]-\hat{N}\}\Psi_\omega(\mathbf{r})=0, \tag{31}$$

where $\mathbf{r}=(x,q)$ is the radius vector in the horizontal plane, $\hat{k}=(\hat{k}_x^2+\hat{k}_q^2)^{1/2}$, while $\hat{N}$ is a self-conjugate linear operator corresponding to a bottom inhomogeneity. However, in three dimensions there is no compact form for $\hat{N}$, valid with any bottom profile. At the moment, there are only approximate expressions $\hat{N}\approx\hat{N}_1+\hat{N}_2+\cdots+\hat{N}_m$, obtained by expansion (up to finite order m) of the vertical velocity at the level $y=0$ in powers of the (relatively small) bottom deviation $\chi(x,q)$ from a constant level $y=-h$. The linear self-conjugate operators $\hat{N}_j$ have the general structure

$$\hat{N}_j=[\cosh(h\hat{k})]^{-1}\hat{S}_j[\cosh(h\hat{k})]^{-1}, \tag{32}$$

with

$$\hat{S}_1=(\boldsymbol{\nabla}\chi\boldsymbol{\nabla}), \tag{33}$$

$$\hat{S}_2=-(\boldsymbol{\nabla}\chi\boldsymbol{\nabla})\left(\frac{\tanh(h\hat{k})}{\hat{k}}\right)(\boldsymbol{\nabla}\chi\boldsymbol{\nabla}), \tag{34}$$

$$\hat{S}_3 = (\nabla\chi\nabla)\left(\frac{\tanh(h\hat{k})}{\hat{k}}\right)(\nabla\chi\nabla)\left(\frac{\tanh(h\hat{k})}{\hat{k}}\right)(\nabla\chi\nabla) + \left(\frac{1}{2}(\nabla\chi^2\nabla)(\nabla\chi\nabla) - \frac{1}{6}(\nabla\chi^3\nabla)\nabla^2\right), \quad (35)$$

and so on, where ∇ is the horizontal gradient (see Appendix A).

Now we are going to calculate ϵ_0, ϵ_1, and ϵ_2. Let us note that with $\epsilon \ll 1$ the four independent eigenfunctions in Bragg resonance are $\Psi_{cc} \approx \cos(\kappa x)\cos(\kappa q)$, $\Psi_{ss} \approx \sin(\kappa x)\sin(\kappa q)$, $\Psi_{cs} \approx \cos(\kappa x)\sin(\kappa q)$, and $\Psi_{sc} \approx \sin(\kappa x)\cos(\kappa q)$. Accordingly, we have for the eigenfrequencies

$$\omega_{cc}^2/g \approx \varkappa \tanh(h\varkappa) + \langle \Psi_{cc}\hat{N}\Psi_{cc}\rangle/\langle \Psi_{cc}^2\rangle, \quad (36)$$

(where $\langle\cdots\rangle$ mean the average value in the horizontal plane), and analogously for ω_{ss}^2 and $\omega_{cs}^2 = \omega_{sc}^2$. Let us introduce shorthand notations for the small quantities $\nu_{cc} \equiv \langle \Psi_{cc}\hat{N}\Psi_{cc}\rangle/[2\varkappa\langle\Psi_{cc}^2\rangle] \ll 1$, and similarly for ν_{ss} and $\nu_{cs} = \nu_{sc}$. Then we have the approximate equalities

$$\omega_{cc} \approx \Omega_*(1 - \epsilon + \nu_{cc}), \quad (37)$$

$$\omega_{ss} \approx \Omega_*(1 - \epsilon + \nu_{ss}), \quad (38)$$

$$\omega_{cs} = \omega_{sc} \approx \Omega_*(1 - \epsilon + \nu_{cs}). \quad (39)$$

These frequencies should be identified with the eigenfrequencies of the linear part of the system (28) and (29), for space-independent solutions:

$$\omega_{(1,1,1,1)} = \Omega_*[(1 - \epsilon_0) + \epsilon_1 + 2\epsilon_2] = \omega_{cc}, \quad (40)$$

$$\omega_{(1,1,-1,-1)} = \Omega_*[(1 - \epsilon_0) + \epsilon_1 - 2\epsilon_2] = \omega_{ss}, \quad (41)$$

$$\omega_{(1,-1,1,-1)} = \Omega_*[(1 - \epsilon_0) - \epsilon_1] = \omega_{cs}, \quad (42)$$

$$\omega_{(1,-1,-1,1)} = \Omega_*[(1 - \epsilon_0) - \epsilon_1] = \omega_{sc}. \quad (43)$$

As a result, we obtain the required formulas for the model parameters:

$$\epsilon_0 \approx \epsilon - \frac{1}{4}(\nu_{cc} + \nu_{ss} + 2\nu_{cs}), \quad (44)$$

$$\epsilon_1 \approx \frac{1}{4}(\nu_{cc} + \nu_{ss} - 2\nu_{cs}), \quad (45)$$

$$\epsilon_2 \approx \frac{1}{4}(\nu_{cc} - \nu_{ss}). \quad (46)$$

With Eqs. (32)–(35), calculation of ν_{cc}, ν_{ss}, and ν_{cs} is straightforward if the function $\chi(x,q)$ contains a finite number of Fourier harmonics; for example,

$$\chi = \frac{\alpha_1}{\kappa}(\cos 2\kappa x + \cos 2\kappa q) + \frac{\alpha_2}{\kappa}\cos 2\kappa x \cos 2\kappa q. \quad (47)$$

Moreover, since $\epsilon \ll 1$, it is possible to simplify the operators $\hat{S}_j$ by writing there $\hat{k}^{-1}$ instead of $[\tanh(h\hat{k})/\hat{k}]$. By doing so and taking into account only $\hat{N}_1$ and $\hat{N}_2$, for the bottom profile (47) we obtain approximately

$$\epsilon_2 \approx -\frac{2\epsilon}{\sqrt{5}}\alpha_1\alpha_2, \quad (48)$$

$$\epsilon_1 \approx \frac{\epsilon}{\sqrt{2}}\alpha_2, \quad (49)$$

$$\epsilon_0 \approx \epsilon\left[1 + \frac{8}{\sqrt{5}}\alpha_1^2 + \left(1 + \frac{1}{2\sqrt{5}}\right)\alpha_2^2\right]. \quad (50)$$

Thus, the expansion $\hat{N} \approx \hat{N}_1 + \hat{N}_2 + \cdots + \hat{N}_m$ is certainly useful for analysis of the case $|\nabla\chi| \ll 1$, but it can hardly be valid for a strongly undulating bed. It should be noted that a global representation of the velocity potential in the form (A1) (see Appendix A) is questionable in the general case. The derivation of $\hat{N}$ for arbitrary $|\nabla b|$, assuming $\epsilon \ll 1$, is an interesting open problem.

It is worth noting that an explicit (though approximate) form of the operator $\hat{N}$ allows us to derive weakly nonlinear equations of motion for water waves over a nonuniform 2D bottom. For example, the Hamiltonian functional [it is the kinetic energy $\mathcal{K}$ plus the potential energy $(g/2)\int \eta^2 d^2\mathbf{r}$] up to the fourth order in terms of the canonically conjugate variables $\eta(\mathbf{r},t)$ and $\psi(\mathbf{r},t)$ is written below:

$$\mathcal{H} \approx \frac{1}{2}\int \{\psi\hat{K}\psi + g\eta^2 + \eta[(\nabla\psi)^2 - (\hat{K}\psi)^2]\}d^2\mathbf{r} + \frac{1}{2}\int [\psi\hat{K}\eta\hat{K}\eta\hat{K}\psi + \eta^2(\hat{K}\psi)\nabla^2\psi]d^2\mathbf{r}, \quad (51)$$

where $\hat{K} \equiv [\hat{k}\tanh(h\hat{k}) + \hat{N}]$ (see Appendix B). It is interesting to note that the bottom inhomogeneity comes into the Hamiltonian through the definition of the operator $\hat{K}$ only. For $\hat{N} = 0$, Eq. (51) coincides with the previously known fourth-order Hamiltonian for water waves at a uniform depth (see, e.g., Ref. [17], and references therein). It is also clear that the coupled-mode system (28) and (29) corresponds to the case $\hat{K} \approx \hat{k}$, when the difference $(\hat{K} - \hat{k})$ is neglected in the third- and fourth-order parts of the Hamiltonian, but is kept in the second-order part. The functional $\mathcal{H}\{\eta,\psi\}$ determines the canonical equations of motion,

$$\eta_t = \frac{\delta\mathcal{H}}{\delta\psi} \approx \hat{K}\psi - (\nabla\eta\nabla)\psi - \hat{K}\eta\hat{K}\psi + \hat{K}\eta\hat{K}\eta\hat{K}\psi + \frac{1}{2}[\hat{K}\eta^2\nabla^2\psi + \nabla^2\eta^2\hat{K}\psi], \quad (52)$$

$$-\psi_t = \frac{\delta \mathcal{H}}{\delta \eta} \approx g\eta + \frac{1}{2}[(\nabla\psi)^2 - (\hat{K}\psi)^2] + (\hat{K}\psi)\hat{K}(\eta\hat{K}\psi) + \eta(\hat{K}\psi)\nabla^2\psi. \tag{53}$$

Numerical simulation of these cubically nonlinear equations, with $\hat{N} \neq 0$, will be an important subject of future research.

Further analytical and computational work is also needed to investigate the formation of vortex structures near the bottom boundary and to evaluate their influence on the free-surface dynamics. In any case, the present results, based on the 2D purely potential theory, deserve attention. Moreover, the author hopes that in a future real-world experiment all the mentioned dissipative processes will be unable to destroy water-wave GSs for a sufficiently long time. Instead, with vortices and breaking wave crests, the predicted phenomenon of standing self-localized water waves over a periodic bed will be found even more rich, interesting, and beautiful.

ACKNOWLEDGMENTS

These investigations were supported by RFBR Grant No. 06-01-00665, by RFBR-CNRS Grant No. 07-01-92165, by the "Leading Scientific Schools of Russia" Grant No. 4887.2008.2, and by the Program "Fundamental Problems of Nonlinear Dynamics" from the RAS Presidium.

APPENDIX A: EXPANSION OF OPERATOR $\hat{N}$

The expansion of $\hat{N}$ in powers of χ is easily obtained from the integral representation of the velocity potential,

$$\Phi(\mathbf{r},y) = \int \left(\phi_{\mathbf{k}} \frac{\cosh k(y+h)}{\cosh kh} + f_{\mathbf{k}} \frac{\sinh ky}{k} \right) e^{i\mathbf{k}\cdot\mathbf{r}} \frac{d^2\mathbf{k}}{(2\pi)^2}, \tag{A1}$$

where $\phi_{\mathbf{k}}$ is the Fourier transform of the velocity potential at $y=0$, and $f_{\mathbf{k}}$ is the Fourier transform of an unknown function $f(\mathbf{r})$ which should be determined by substitution of Eq. (A1) into the bottom boundary condition

$$(\partial\Phi/\partial y - \nabla\chi\cdot\nabla\Phi)|_{y=-h+\chi} = 0. \tag{A2}$$

The resulting integral equation can be represented as follows:

$$-\nabla\cdot\int f_{\mathbf{k}} \frac{i\mathbf{k}\cosh[k(\chi(\mathbf{r})-h)]}{k^2} \exp(i\mathbf{k}\cdot\mathbf{r}) \frac{d^2\mathbf{k}}{(2\pi)^2} - \nabla\cdot\int \phi_{\mathbf{k}} \frac{i\mathbf{k}\sinh[k\chi(\mathbf{r})]}{k\cosh(kh)} \exp(i\mathbf{k}\cdot\mathbf{r}) \frac{d^2\mathbf{k}}{(2\pi)^2} = 0. \tag{A3}$$

It can be formally solved for $f(\mathbf{r})$ by expanding Eq. (A3) in powers of χ and assuming $f=f_1+f_2+\cdots$. For instance, Eq. (A3) with third-order accuracy is written below:

$$\left[1 + (\nabla\chi\nabla)\left(\frac{\tanh(h\hat{k})}{\hat{k}}\right) - \left(\nabla\frac{\chi^2}{2}\nabla\right)\right][\cosh(h\hat{k})]f = \left[(\nabla\chi\nabla) - \left(\nabla\frac{\chi^3}{6}\nabla\right)\nabla^2\right][\cosh(h\hat{k})]^{-1}\phi. \tag{A4}$$

As a result, we obtain an approximate solution $f \approx (\hat{N}_1 + \hat{N}_2 + \hat{N}_3)\phi$, where the operators $\hat{N}_1$, $\hat{N}_2$, and $\hat{N}_3$ are given by Eqs. (32)–(35). A linearized system describing the free-surface dynamics is

$$-\psi_t = g\eta, \quad \eta_t = [\hat{k}\tanh(h\hat{k})]\psi + f, \tag{A5}$$

where $\psi(\mathbf{r}) = \Phi(\mathbf{r}, \eta(\mathbf{r}))$ is the surface value of the velocity potential (in the linear approximation $\psi \approx \phi$). It gives us Eq. (31) for the eigenfunctions Ψ_ω corresponding to some fixed frequency ω.

APPENDIX B: HAMILTONIAN OF WATER WAVES UP TO THE FIFTH ORDER

An approximate Hamiltonian of water waves can be easily derived by writing the kinetic energy of potential three-dimensional motion of an ideal fluid in the form

$$\begin{aligned}\mathcal{K} &= \frac{1}{2}\int d^2\mathbf{r}\int_{-h+\chi(\mathbf{r})}^{\eta(\mathbf{r})} [(\partial\Phi/\partial y)^2 + (\nabla\Phi)^2]dy \\ &= \frac{1}{2}\int \psi[\partial\Phi/\partial y - \nabla\eta\cdot\nabla\Phi]|_{y=\eta} d^2\mathbf{r} \\ &= \frac{1}{2}\int \nabla\psi\cdot\int \left(\phi_{\mathbf{k}} \frac{i\mathbf{k}\sinh\{k[\eta(\mathbf{r})+h]\}}{k\cosh(kh)} + f_{\mathbf{k}} \frac{i\mathbf{k}\cosh[k\eta(\mathbf{r})]}{k^2}\right)\exp(i\mathbf{k}\cdot\mathbf{r})\frac{d^2\mathbf{k}}{(2\pi)^2} d^2\mathbf{r} \\ &= \frac{1}{2}\int \left(\psi\hat{K}\phi + \eta\nabla\psi\cdot\nabla\phi + \frac{\eta^2}{2}\nabla\psi\cdot\nabla\hat{K}\phi - \frac{\eta^3}{6}\nabla\psi\cdot\nabla(\nabla^2\phi) + \cdots\right) d^2\mathbf{r},\end{aligned} \tag{B1}$$

with the subsequent substitution

$$\phi \approx \psi - \eta\hat{K}\psi + \eta\hat{K}\eta\hat{K}\psi + \frac{\eta^2}{2}\nabla^2\psi - \eta\hat{K}\left(\eta\hat{K}\eta\hat{K}\psi + \frac{\eta^2}{2}\nabla^2\psi\right) - \frac{\eta^2}{2}\nabla^2\eta\hat{K}\psi + \frac{\eta^3}{6}\nabla^2\hat{K}\psi. \tag{B2}$$

The approximate equality (B2) follows from an expansion of Eq. (A1): $\psi \approx [1 + \eta\hat{K} - (\eta^2/2)\nabla^2 - (\eta^3/6)\nabla^2\hat{K}]\phi$. Thus,

$$\begin{aligned}\mathcal{K} = \frac{1}{2}\int \Bigg\{ &\psi\hat{K}\left[\psi - \eta\hat{K}\psi + \eta\hat{K}\eta\hat{K}\psi + \frac{\eta^2}{2}\nabla^2\psi - \eta\hat{K}\left(\eta\hat{K}\eta\hat{K}\psi + \frac{\eta^2}{2}\nabla^2\psi\right) - \frac{\eta^2}{2}\nabla^2\eta\hat{K}\psi + \frac{\eta^3}{6}\nabla^2\hat{K}\psi\right] \\ &+ \eta\nabla\psi\cdot\nabla\left(\psi - \eta\hat{K}\psi + \eta\hat{K}\eta\hat{K}\psi + \frac{\eta^2}{2}\nabla^2\psi\right)\end{aligned}$$

$$+\frac{\eta^2}{2}\nabla\psi\cdot\nabla\hat{K}(\psi-\eta\hat{K}\psi)-\frac{\eta^3}{6}\nabla\psi\cdot\nabla(\nabla^2\psi)+\cdots\Bigg\}d^2\mathbf{r}. \tag{B3}$$

After simplifying, we obtain $\mathcal{H}=\frac{1}{2}\int\{\psi\hat{K}\psi+g\eta^2+\eta[(\nabla\psi)^2-(\hat{K}\psi)^2]\}d^2\mathbf{r}+\mathcal{H}^{(4)}+\mathcal{H}^{(5)}+\cdots$, where

$$\mathcal{H}^{(4)}=\frac{1}{2}\int[\psi\hat{K}\eta\hat{K}\eta\hat{K}\psi+\eta^2(\hat{K}\psi)\nabla^2\psi]d^2\mathbf{r}, \tag{B4}$$

$$\mathcal{H}^{(5)}=\frac{1}{2}\int\left(\frac{\eta^3}{6}(\hat{K}\psi)\nabla^2\hat{K}\psi-\psi\hat{K}\eta\hat{K}\eta\hat{K}\eta\hat{K}\psi-\frac{\eta^3}{3}(\nabla^2\psi)^2-\eta^2(\hat{K}\eta\hat{K}\psi)\nabla^2\psi-\frac{\eta^2}{2}(\hat{K}\psi)\nabla^2(\eta\hat{K}\psi)\right)d^2\mathbf{r}. \tag{B5}$$

In the same manner, it is also possible to derive the Hamiltonian with a higher-order accuracy.

[1] W. Chen and D. L. Mills, Phys. Rev. Lett. **58**, 160 (1987).
[2] A. B. Aceves and S. Wabnitz, Phys. Lett. A **141**, 37 (1989).
[3] B. J. Eggleton, R. E. Slusher, C. M. de Sterke, P. A. Krug, and J. E. Sipe, Phys. Rev. Lett. **76**, 1627 (1996).
[4] D. N. Christodoulides and R. I. Joseph, Phys. Rev. Lett. **62**, 1746 (1989).
[5] T. Peschel, U. Peschel, F. Lederer, and B. A. Malomed, Phys. Rev. E **55**, 4730 (1997).
[6] I. V. Barashenkov, D. E. Pelinovsky, and E. V. Zemlyanaya, Phys. Rev. Lett. **80**, 5117 (1998).
[7] A. De Rossi, C. Conti, and S. Trillo, Phys. Rev. Lett. **81**, 85 (1998).
[8] C. Conti, S. Trillo, and G. Assanto, Phys. Rev. Lett. **85**, 2502 (2000).
[9] T. Iizuka and C. Martijn de Sterke, Phys. Rev. E **61**, 4491 (2000).
[10] C. Conti and S. Trillo, Phys. Rev. E **64**, 036617 (2001).
[11] K. W. Chow, I. M. Merhasin, B. A. Malomed, K. Nakkeeran, K. Senthilnathan, and P. K. A. Wai, Phys. Rev. E **77**, 026602 (2008).
[12] N. K. Efremidis and D. N. Christodoulides, Phys. Rev. A **67**, 063608 (2003).
[13] D. E. Pelinovsky, A. A. Sukhorukov, and Yu. S. Kivshar, Phys. Rev. E **70**, 036618 (2004).
[14] M. Matuszewski, W. Krolikowski, M. Trippenbach, and Y. S. Kivshar, Phys. Rev. A **73**, 063621 (2006).
[15] V. P. Ruban, Phys. Rev. E **77**, 055307(R) (2008).
[16] V. P. Krasitskii, J. Fluid Mech. **272**, 1 (1994).
[17] V. Zakharov, Eur. J. Mech. B/Fluids **18**, 327 (1999).
[18] V. P. Ruban, Phys. Rev. E **70**, 066302 (2004).
[19] M. Onorato, A. R. Osborne, and M. Serio, Phys. Rev. Lett. **96**, 014503 (2006).
[20] V. P. Ruban, Phys. Lett. A **340**, 194 (2005).
[21] V. P. Ruban, Phys. Rev. E **77**, 037302 (2008).
[22] T. Hara and C. C. Mei, J. Fluid Mech. **178**, 221 (1987).